Original
Paper

phys. stat. sol. (b) **244**, No. 4, 1363 – 1375 (2007) / **DOI** 10.1002/pssb.200642373

Bleaching kinetics of indoly-benzylfulgimide in PMMA

Romano A. Rupp[*,1,4], **Yuan Zheng**[2], **Yingli Wang**[2], **Weibin Dong**[2], **Neimule Menke**[2], **Baoli Yao**[2], **Wei Zhao**[2], **Yi Chen**[3], **Meigong Fan**[3], **Jinjun Xu**[4], and **Martin Fally**[1]

[1] Institute for Experimental Physics, University of Vienna, Boltzmanngasse 5, 1090 Wien, Austria
[2] State Key Laboratory of Transient Optics Technology, Xian Institute of Optics and Precision Mechanics, Chinese Academy of Sciences, Xian 710068, P.R. China
[3] Technical Institute of Physics and Chemistry, Chinese Academy of Sciences, Beijing 100101, P.R. China
[4] Photonics Research Center, College of Physical Science, Nankai University, Tianjin 300071, P.R. China

Received 30 June 2006, revised 14 September 2006, accepted 4 October 2006
Published online 12 December 2006

PACS 33.20.Kf, 78.40.–q, 82.50.Hp, 82.50.Nd

Indoly-benzylfulgimide belongs to the photochromic fulgide family and follows photochemical first order kinetics. Its bleaching kinetics is investigated at 633 nm and 640 nm by spectroscopy, by the time dependence of transmission and of diffraction from holographically induced gratings. The non-exponential decay law resulting for diffraction experiments with a Gaussian beam profile is calculated and verified experimentally. For a quasi-homogeneous beam profile the time constant determined from diffraction decay is half the one for absorbance decay. The photochemical reaction rate of indoly-benzylfulgimide in PMMA is (3.9 ± 0.3) cm^2/J at 650 nm.

1 Introduction

By photon irradiation aryl-fulgides and its modifications (for brevity also called fulgides in the following) may be reversibly switched between two isomers, namely a thermally stable ground state, the so-called E-form, and the so-called C-form which can be either thermally metastable or stable. The molecular process of switching takes place within approximately 10^{-11} s [1]. The (closed or) C-form having its name from the ring closure of the 1,3,5-hexatriene structure results from photoinduced 6π electrocyclization [2]. In this paper we discuss only fulgides with heteroaromatic rings which exhibit thermally stable C-isomers. The spectrum of the “colorless” E-isomer differs from the one of the “colored” C-isomer by characteristic vibrational bands in the infrared [3, 4] as well as by electronic excitation and electronic transfer bands. The latter are in the ultraviolet (UV) for the E-isomer and in the visible for the C-isomer. In addition a so-called Z-isomer exists which can be generated from the E-isomer by UV irradiation. Since the latter photochemical reaction can be effectively suppressed by embedding fulgide molecules into a sufficiently rigid matrix [5], optically switchable bistable molecular systems may be achieved on the basis of heteroaromatic fulgides.

For applications in holography, holographic interferometry, optical information storage [6], integrated optics [7, 8] or optical telecommunication, fulgides are incorporated into solid host materials such as polymers or other glasses. Roughly speaking, the effects caused by switching between the E- and C-forms may be distinguished according to the following classification: (1) Intrinsic effects arising from the differing physical properties of the isomers. (2) Extrinsic effects by reaction of the host matrix on the

[*] Corresponding author: e-mail: romano.rupp@univie.ac.at

photoinduced exchange of the isomers. (3) Non-reversible effects (aging or fatigue) caused by reactions of the fulgide molecules upon non-reversible rearrangements of the matrix or by chemical reactions with the matrix or the environment.

Changes of the absorption spectra as well as the pertinent (because of Kramers–Kronig relationship) changes of the refractive index belong mainly to the first class. The fact that switching is fast [1] and reversible makes fulgides attractive photochromic and photorefractive systems for many applications. Apart from that, photoswitching between both isomers may influence the luminescence or liquid crystalline properties of specially designed systems. Fulgide systems may be ordered by poling in an electric field under irradiation and exhibit birefringence, dichroism or nonlinear optical properties because of the dipolar character of the molecules. Likewise, fulgide systems can be ordered by optical polarization resulting in birefringence and dichroism [9]. Since the E-form is chiral, the capabilities for optically switchable circular dichroism and circular birefringence (optical activity) may be exploited. In this paper we report on a fulgide modification, namely 3-indoly-benzylfulgimide, which was doped into a PMMA matrix. We investigate the kinetics resulting from irradiation with a (quasi-)homogeneous beam profile theoretically as well as by spectroscopy, transmission and diffraction experiments.

2 Experimental

A solution was prepared by dissolving 10 wt% PMMA as well as 1 wt% (sample named 6a) and 2 wt% (samples named 6b and c) 3-indoly-benzylfulgimide (Fig. 1) in cyclohexanone. The film is obtained by spreading several drops of the solution on a glass substrate (∅ 25 mm × 1.5 mm) and subsequent drying in air. The thicknesses of two samples were determined to be 10 μm and 13 μm by microscopy of the cross section. As all samples were obtained by the same procedure, we assume in the following that they have a nominal thickness of $d = (12 \pm 3)$ μm (corroborated by findings presented in Section 4). The final concentration in the PMMA matrix was 10 wt% (≈2.7 at%) 3-indoly-benzylfulgimide for sample 6a, and 20 wt% (≈5.4 at%) for the samples 6b and c. Samples 6a and b were prepared 21 months before our optical experiments and were already used several times for optical experiments. Sample 6c was obtained in virgin state and studied within two weeks after preparation. Polarized and non-polarized absorption spectra of the samples were measured with the spectrometer UV-31101 (Shimadzu Inc.).

The experimental set-up for transmission and holographic measurements is shown in Fig. 2. A typical experimental cycle of the measurements consist of the following steps: (1) Transfer of the fulgimide molecules into C-isomers by irradiation at 405 nm. (2) Only in case of holographic measurements: Generation of holographic gratings at 650 nm by partial transfer of the molecules into E-isomers. (3) Bleaching at 633 nm or 650 nm by transfer to E-isomers using (quasi-)homogenous beams or beams with Gaussian profile. Thereby the kinetics of the bleaching process is deduced from monitoring the decay of the first order diffraction or from the increase of transmission.

(1) Prior to the begin of all bleaching experiments the sample was irradiated for 10–20 min (depending on the sample) with opened iris diaphragm (Fig. 2) using a diode laser ($\lambda \approx 405$ nm, intensity approximately 75 mW/cm^2, polarization in plane of incidence) until the photostationary state was reached. In order to achieve a homogeneous initial distribution the beam was expanded by a lens to a diameter of approximately 10 mm.

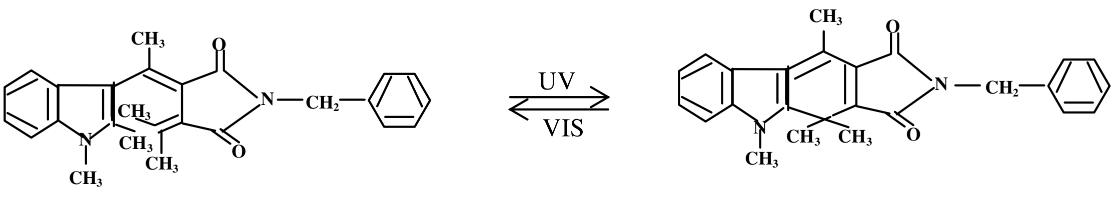

Fig. 1 Chemical structure and photoswitching of 3-indoly-benzylfulgimide. Left: E-form with open ring, right: C-form with closed ring.

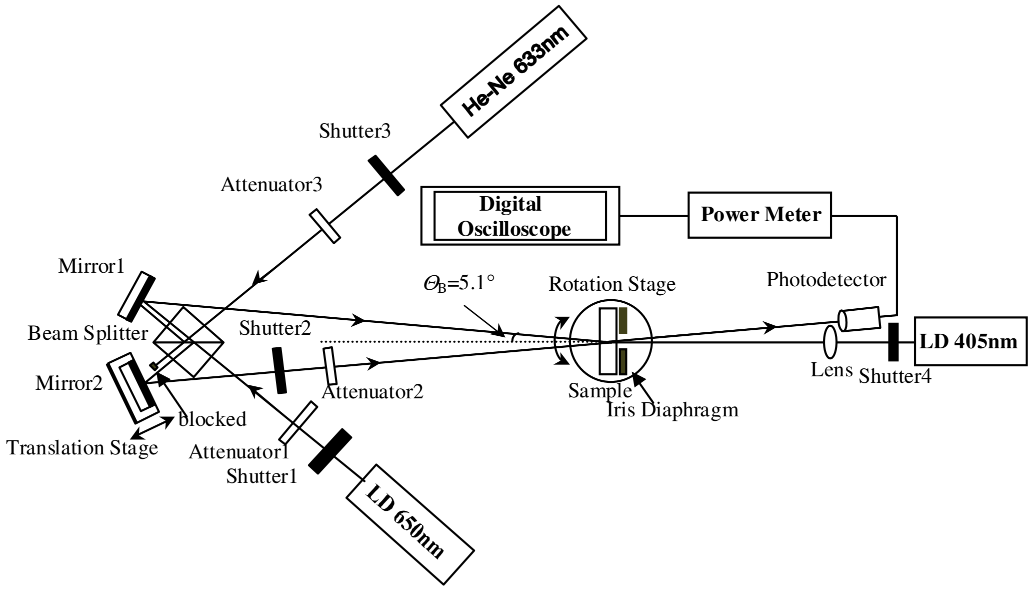

Fig. 2 Optical set-up for measurements of the kinetics by transmission and holographic probing. Writing: laser diode (LD) at 650 nm, reading: He–Ne laser at 633 nm, erasure: laser diode (LD) at 405 nm.

(2) The grating, whose decay kinetics was to be monitored, was first holographically written in the bleaching mode with a diode laser at a wavelength of 650 nm. The beam was collimated by a lens and had an elliptical profile with about $3 \times 10\ \text{mm}^2$ along the main axes with polarization along the short axis, i.e., parallel to the plane of incidence. Adjustment of coherence was made by creating a Michelson interferometer. To that purpose the mirrors were first adjusted perpendicularly to the faces of the beamsplitter cube. The interference fringes were tuned for optimum contrast by moving one of the mirrors with a translation stage. Finally the mirrors were rotated for optimum overlap at the sample positioned on the symmetry line between both mirrors intersecting at an angle $2\theta_B = 180$ mrad corresponding to a grating spacing $\Lambda = 3.5$ µm (±5%). The intersection area was defined by closing the iris diaphragm (Fig. 2) to a diameter of approximately 4 mm. Within one series of kinetic measurements as a function of intensity the exposure used to generate the grating was approximately the same.

(3) For read-out of the holograms and for the transmission measurements either one of the writing beams at 650 nm or the beam of an unpolarized He–Ne laser at $\lambda = 633$ nm was used. These monitoring beams had a (quasi-)homogeneous or a Gaussian profile at the input plane, respectively. While monitoring they induce in the same time the kinetics of the photochemical transfer to the E state which we are going to study. In diffraction experiments the angle of incidence was $\theta \approx 90$ mrad (±5%), i.e. the same as for the writing beams and thus slightly off the Bragg angle for 633 nm. Nevertheless, we are still sufficiently close to the Bragg angle at 633 to ignore off-Bragg corrections. The reason is that the quality factor for read-out was determined to be $Q = \lambda d_g/\Lambda^2 \leq 0.6$ in our case (i.e. Raman–Nath regime). Here d_g denotes the thickness of the grating. A calibrated power meter (United Detector Company, model 11A) equipped with a silicon photodiode and a filter for spectrally flat radiation measurements was used. For the determination of the incident intensity I_0 the calibration factors of the measurement system as well as reflections coefficient of the input face of the sample were taken into account. By this procedure the accuracy of the absolute intensities is estimated to be better than 10%. As concerns a possible systematic error, we depend on the calibration established by the manufacturer of the instrument. All kinetic erasure/bleaching experiments were performed at a laboratory temperature of 25–27 °C. The data were digitized by a storage oscillograph and processed by a computer.

3 Theory

3.1 Photochemistry and local optical constants

For a fully bistable fulgide system and neglecting side reactions like E-Z-isomerization or aging effects the photochemical reaction is local and follows first order kinetics:

$$\begin{aligned} \frac{\mathrm{d}C}{\mathrm{d}Q} &= -\gamma_{\mathrm{C}} C + \gamma_{\mathrm{E}} E\,, \\ \frac{\mathrm{d}E}{\mathrm{d}Q} &= -\gamma_{\mathrm{E}} E + \gamma_{\mathrm{C}} C\,. \end{aligned} \tag{1}$$

Here C and E are the concentrations of the C- and E-isomers, respectively, and Q denotes the local exposure that is related to the intensity I by $\dot{Q} = I$. Dots denote time derivatives. In Eq. (1) irradiation with mono-energetic photons is assumed. The photochemical reaction constants γ_{C} and γ_{E} depend on photon energy which is expressed in the following in terms of the so-called wavelength λ of the photon. Upon irradiation the concentrations will change until a photostationary state (index ∞) is reached at the concentration ratio given by $C_\infty/E_\infty = \gamma_{\mathrm{E}}/\gamma_{\mathrm{C}}$. The solution of the above system of equations is given by

$$\Delta C(Q) = \Delta C_0 \exp(-\gamma Q). \tag{2a}$$

Here $\Delta C(Q) = C(Q) - C_\infty$ and $\Delta C_0 = C_0 - C_\infty$ denote the so-called excess concentrations, i.e., the deviations from the equilibrium concentration $C_\infty = C(Q \to \infty)$, $C_0 = C(Q = 0)$ is the initial concentration, $\gamma = \gamma_{\mathrm{C}} + \gamma_{\mathrm{E}}$ is the (effective) photochemical reaction constant, and a similar equation holds for $\Delta E(Q)$.

For simplicity let us assume constant intensity, i.e. $Q = It$, where t denotes time. By defining the effective photochemical rate constant $k = \gamma I$, Eq. (2) then predicts an exponential decay

$$\Delta C(t) = \Delta C_0 \exp(-kt) \tag{2b}$$

of excess concentration with a decay time $\tau = k^{-1}$. Strictly speaking, the intensity is nowhere constant in time within a photochromic medium with the possible exception of the entrance face. For a theory that takes this fact into account we refer to Ref. [10]. Here we use Eq. (2b) only as an illustrative approximation and as a starting point for discussion.

The local contributions of the isomers to the absorption spectrum and to the refractive index are given by:

$$\begin{aligned} \Delta\alpha &= \sigma_{\mathrm{C}} C + \sigma_{\mathrm{E}} E \\ \Delta n &= R_{\mathrm{C}} C + R_{\mathrm{E}} E\,. \end{aligned} \tag{3}$$

Here $\sigma_{\mathrm{C,E}}$ are the absorption cross sections and $R_{\mathrm{C,E}}$ the effective refractivities of the C- and E-isomers, respectively. In $R_{\mathrm{C,E}}$ we have lumped together the molecular refractivities and a factor depending on the refractive index n of the host matrix (which is suggested, e.g., by the Clausius–Mossotti relationship) into one single constant, namely the effective refractivities $R_{\mathrm{C,E}}$. It goes without saying that all quantities in Eq. (3) with the exception of the concentrations C and E depend on the wavelength λ. The experiments to be discussed in this paper were performed at wavelengths where σ_{E} and R_{E} can be neglected.

3.2 Bleaching kinetics from transmission and holographic read-out measurements

The bleaching kinetics of the C-isomer is inferred from transmission or diffraction experiments. We first consider the ideal case where bleaching is performed by irradiation of the input face with homogeneously distributed light of intensity I_0. The case of a Gaussian beam profile will be discussed below.

In transmission experiments the absorbance $A = -\lg(I_t/I_0)$ or $A_e = -\ln(I_t/I_0)$, respectively, of a sample of thickness d is determined, where I_0 is the intensity measured at the input face ($z = 0$) of the sample and

I_t is the transmitted intensity measured behind the output face ($z = d$). The absorbance kinetics can be described by [10]:

$$\ln\left(\frac{\Delta A(t)}{\Delta A(0)}\right) = \ln\left(\frac{A(t) - A(\infty)}{A(0) - A(\infty)}\right) = -k_A t - f(t)\,, \tag{4}$$

Here $\Delta A(t)$ is the difference of the absorbance $A(t)$ of the transfer band of the C-isomer at time t and of the absorbance $A(\infty)$ for $t \to \infty$, i.e. for the fully bleached state. With increasing absorbance the local intensity decreases with penetration depth resulting in

$$k_A = \tau_A^{-1} = k_0\,[1 - \exp(-\Delta A_{e0})]/\Delta A_{e0} = \gamma I_0[1 - \exp(-\Delta A_{e0})]/\Delta A_{e0}\,. \tag{5}$$

The quantity $k_0 = \gamma I_0$ is the effective photochemical rate constant at the input face ($z = 0$). The function $f(t)$ describes nonlinear deviations of the absorbance kinetics and vanishes for $t \to 0$ [10]. Essentially, Eq. (5) may be understood as replacing the incident intensity I_0 by an average intensity inside the sample which is reduced by a factor depending on the initial absorbance $\Delta A_0 = \Delta A(0)$. Based on our findings in [10] we determine k_A for our experiments from the initial part of the absorbance decay where nonlinear deviations are still negligible.

In order to define the quantities needed to analyze our diffraction experiments we repeat in short the basic relationships for a mixed absorption/refraction grating of thickness d in the limiting case of small diffraction efficiency and vanishing absorbance. For simplicity we assume that a concentration grating has been generated by holographic recording from which only the first order harmonics

$$C(x) = C_0 + C_1 \cos(Kx), \tag{6}$$

is of importance. This is the case if read out is performed at or sufficiently close to the nominal Bragg angle $\theta_B = \arcsin(\lambda/2\Lambda)$. During bleaching with a homogeneous light distribution both components, C_0 and C_1, decay exponentially with time according to Eq. (2). This results in a decay of the mixed absorption/refractive index grating (Eq. (3)):

$$\begin{aligned} \Delta\alpha(x,t) &= (\Delta\alpha_1(t)/2)\cos(Kx)\,,\\ \Delta n(x,t) &= \Delta n_1(t)\cos(Kx)\,. \end{aligned} \tag{7}$$

The conditions of our experiments are such that we are within or close to the thin grating regime ($Q < 1$). Then the first order diffraction efficiency is given by [11]:

$$\eta \approx [(\Delta\alpha_1(t)/4)^2 + (\pi\,\Delta n_1(t)/\lambda)^2]\, d_g^2 \exp(-\alpha_0 d)\,. \tag{8}$$

Here α_0 denotes the average absorption and the factor 1/4 occurs because $\Delta\alpha_1$ refers to the total absorption change (and not to the modulation amplitude), i.e., refers to the intensity (and not amplitude) decay. Hence we expect in first approximation and for the simple case where $\Delta n_1(t)$ and $\Delta\alpha_1(t)$ are proportional to $C(t) \propto \exp(-t/\tau)$ that the diffraction efficiency and the diffracted intensity I_d decay approximately exponentially with

$$\eta \propto I_d \propto \exp(-t/\tau_d) \tag{9}$$

with the time constant $\tau_d = \tau_A/2$. Here again we have taken into account that the effective intensity is reduced by a factor $[1 - \exp(-\Delta A_{e0})]/\Delta A_{e0}$ with respect to the incident intensity I_0.

3.3 Effect of a Gaussian beam profile on the kinetics of holographic decay

In cases where the photochemical bleaching kinetics is inferred from monitoring the decay of holographic gratings, bleaching is for simplicity often induced by the read-out beam itself. We will investigate here the resulting kinetics of holographic decay assuming a Gaussian beam profile and first order kinetics of the photochemical reaction. Thereby we replace γ by γ_A to account for the decay of intensity in z-direction and presume for the plane transverse to it that the initial grating amplitude is homogeneous. The symmetry of the problem suggests the choice of the cylindrical coordinates ρ and z. The Gaussian profile is given by:

$$I(\rho,0) = I_{\max} \exp(-\rho^2/w^2)\,. \tag{10}$$

Here w is a parameter characterizing the width of the beam. At the input plane the relationship between the total power and the maximum intensity is given by $P_0 = \pi w^2 I_{\max}$. Here πw^2 defines the effective cross section of the beam. Even though the local photochemical kinetics is of first order, the consequence of the intensity profile is that the kinetics proceeds faster in the center of the beam and slower at the outskirts. It is therefore obvious that the diffracted power will not follow an exponential time law. The diffracted power is given by

$$\begin{aligned} P_d(t) &= \int_0^\infty \eta(\rho,t)\, I(\rho,t)\, 2\pi\rho \,\mathrm{d}\rho \\ &\propto \int_0^\infty (\Delta C(\rho,t))^2 \exp(-\rho^2/w^2)\, \rho \,\mathrm{d}\rho \\ &\propto \int_0^\infty \exp(-2\gamma_A t I_{\max} \exp(-\rho^2/w^2)) \exp(-\rho^2/w^2)\, \rho\, \mathrm{d}\rho\,, \end{aligned}$$

with the final result

$$P_d(t) \propto \frac{1-\exp(-t/\tau_d)}{t/\tau_d}\,. \tag{11}$$

Here we have defined $\tau_d = (2\gamma_A I_{\max})^{-1}$. For $t/\tau_d \to \infty$ this function decays like $(t/\tau_d)^{-1}$ and for $t/\tau_d \to 0$ like $\exp(-t/2\tau_d) = \exp(-t/\tau_A)$ with $\tau_A = (\gamma_A I_{\max})^{-1}$. The latter is a remarkable coincidence, namely that a single exponential fit to the initial part of Eq. (11) would result in the same time constant as obtained from transmission experiments with a (quasi-)homogeneous beam profile of intensity $I_{\max}$.

We would like to draw attention to the fact that the kinetics of holographic decay according to Eq. (11) does not depend on the width parameter w. This means that by using a more expanded Gaussian beam one does not approach the limiting case of single exponential kinetics of a homogeneous beam profile – unless the Gaussian beam profile is truncated by a diaphragm or by the size of the sample. This underlines the astonishingly general validity of Eq. (11) for experiments with Gaussian beam profile.

4 Experimental results

4.1 Spectroscopy

Sample 6c was colored until steady state by irradiation at 650 nm with a light polarization parallel to the plane of incidence (π-polarized). Subsequent π- and σ-polarized absorption spectra did not show any significant difference, in particular, light-induced dichroism [9] seems to be absent or very weak. Therefore the following results refer to non-polarized absorption spectra.

Two bands can be seen in the absorption spectra shown in Fig. 3a–c: the one centered at 366 nm is characteristic for E-isomers, and the one centered at 576 nm for C-isomers. Figure 3a confirms that in the virgin state all fulgimide molecules are present as E-isomers and that complete bleaching by irradiation with red light is possible even 21 months after sample preparation, i.e. the C-isomers can be switched back completely at any time. Hence we conclude that $\gamma_E(633\ \mathrm{nm}) \approx 0$ holds for the photochemical rate constant. The absorption cross section of the dye molecules can be estimated from the spectrum taken

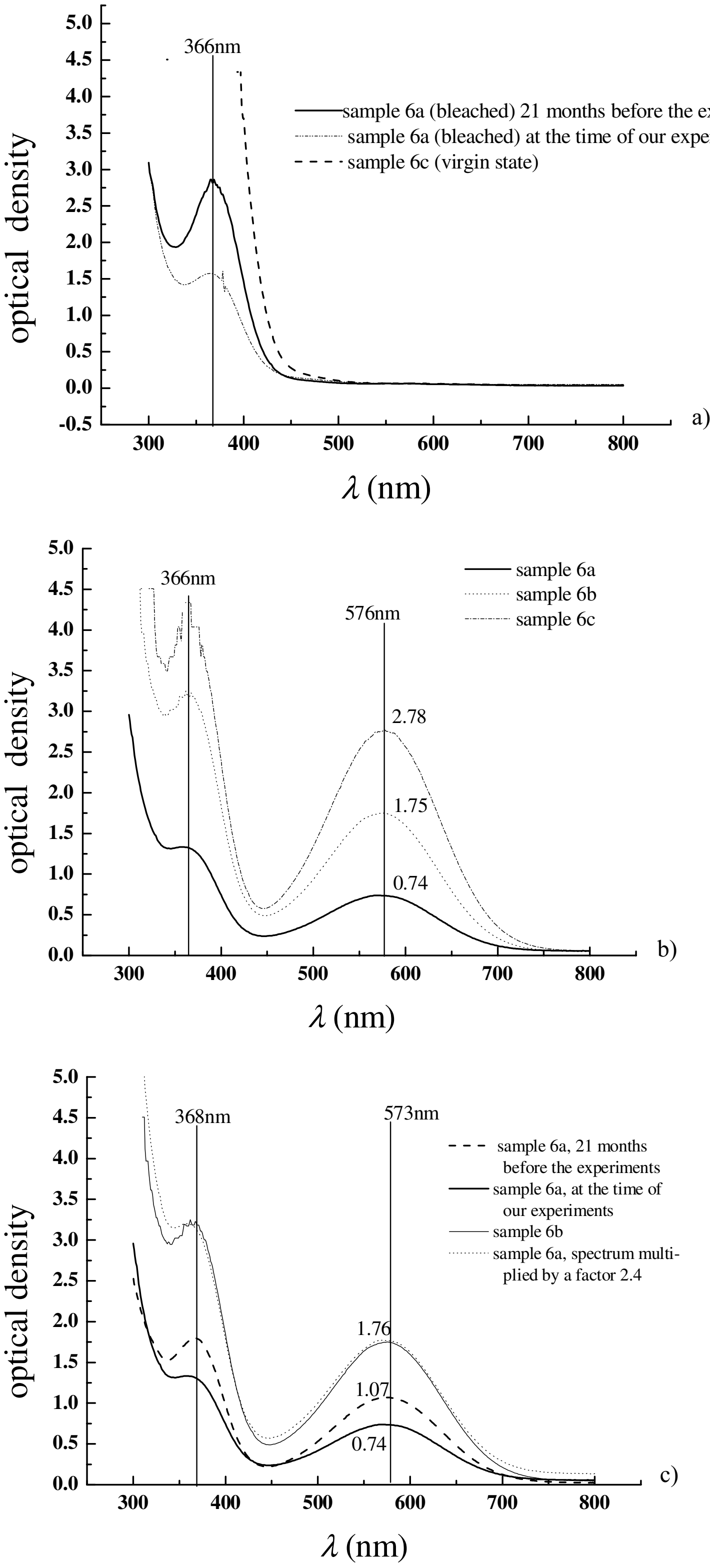

Fig. 3 Unpolarized optical spectra of indoly-benzylfulgimide in PMMA. (a) Spectrum of sample 6c immediately after preparation (virgin state), spectrum of sample 6a in bleached state (after irradiation with red light, spectrum recorded 21 months before our experiments). (b) Colored state (after irradiation with 405 nm): Comparison of samples 6a–c. (c) Colored state: (i) comparison of the present spectrum of sample 6a with the one taken 21 months before; (ii) present spectrum of sample 6b compared with the one of 6a multiplied by a factor 2.4.

shortly after preparation of sample 6a (i.e., 21 months before our experiments) and using the volume of sample 6a to calculate the volume concentration F of the fulgimides at preparation time. We obtain $\sigma(366\text{ nm}) \approx \alpha(366\text{ nm})/F \approx 2 \times 10^{-17}\text{ cm}^2$.

Figure 3b compares absorption spectra of samples 6a–c after coloration at 405 nm until stationary state. The non-vanishing absorption peak at 366 nm proves that complete transfer E $\rightarrow$ C is not possible. Instead, a photostationary state is reached. Comparing the peak at 366 nm in Fig. 3a and c one may estimate that approximately 1/3 of the molecules are transferred to the C-isomers for sample 6a in the photostationary state. As a consequence, we have for the absorption cross sections at the absorption maxima the relationship $\sigma(366\text{ nm}) \approx 0.8 \times \sigma(576\text{ nm})$. Since the optical densities (OD) at the peak maxima are proportional to the saturation concentrations, we may calculate the ratio of the photochemical reaction constants of indoly-benzylfulgimide in PMMA at 405 nm. For the samples 6a and b we consistently obtain: $\gamma_E(405\text{ nm})/\gamma_C(405\text{ nm}) = C_\infty/E_\infty \approx 0.8 \times \text{OD}(576\text{ nm})/\text{OD}(366\text{ nm}) = 0.44$. The value for sample 6c cannot be determined precisely because the maximum was out of the range of our spectrometer, but it is approximately 0.48.

Figure 3c compares the spectra of the colored state of sample 6a measured at the time of this investigation and 21 months before. First of all, we note, that the ratio of the photochemical rate constants (≈ 0.44) has practically not changed within 21 months. However, both peaks, namely the one proportional to the concentration of E-isomers and the one of C-isomers, have diminished by the same fraction of roughly 30%. Obviously, this fraction of fulgimide molecules has leaked out of the bistable E/C-isomeric system either by transforming into Z-isomers or undergoing other chemical reactions, e.g., with the host matrix. This aging process represents a serious degradation of the PMMA:fulgimide system.

A comparison of the spectra of sample 6a, multiplied by a factor 2.4, with the one of sample 6b is made in Fig. 3c and confirms that the chemical composition of both samples is still nearly identical even 21 months after preparation. A slightly enhanced background in sample 6a indicates somewhat higher scattering of the matrix. The ratio of the dye concentrations of sample 6b and 6a is 2.0, while the ratio at the absorption peaks is 2.4. This may be explained by sample 6a having a thickness which is about 20% smaller than the one of sample 6b. If we correct, on the other hand, the value OD = 1.75 at the C-isomer peak of sample 6b by the aging fraction of 30%, approximately the same value is obtained for sample 6c having the same dye concentration. Both observations imply that the sample preparation technique results in samples of nearly the same thicknesses within ±20%.

4.2 Kinetics

First we wanted to check the relationship between the time constant τ_A determined from absorbance decay and τ_d determined from the decay of the diffracted intensity during bleaching. In order to obtain consistent results it turned out to be important that the values were measured at the same conditions, in particular at exactly the same intensity with a beam profile as homogeneous as possible. Further the data have to be treated exactly the same. Therefore we proceeded as follows: After having written holographic gratings with an exposure of approximately 0.51 J/cm^2 into sample 6c, the sample was irradiated by only one read-out beam and the transmitted as well as the diffracted powers (P_t and P_d, respectively) were measured as a function of time. Typical plots of ln (P_t/mW) and of the diffracted intensity I_d are shown in Fig. 4a and b, respectively, for $\lambda = 650$ nm and a readout intensity of 32 mW/cm^2. The data were fitted in both cases by a single exponential function. If we compare now both time constants we indeed find that $\tau_d \approx \tau_A/2$.

The reciprocal of the time constant τ_A from transmission and of $2\tau_d$ obtained from single exponential fits are plotted in Fig. 5 as a function of the absolute intensities in order to obtain the photochemical rate constants. First of all, we note that the slopes in Fig. 5a are practically identical within the error bars. Again this confirms our theoretical result, namely that the time constant τ_d of the diffraction kinetics is only half of the time constant $\tau_A = (\gamma_A I_0)^{-1}$ of the transmission kinetics. Fitting straight lines to the data we obtain from transmission as well as diffraction kinetics the same value for the slope, namely (1.2 ± 0.1) cm^2/J. Using the initial absorbance $\Delta A_0 = 3.1$ (from 1.35 for the optical density at $\lambda = 650$ nm) the photochemical rate constant is calculated to be $\gamma(650\text{ nm}) = (3.9 \pm 0.3)$ cm^2/J.

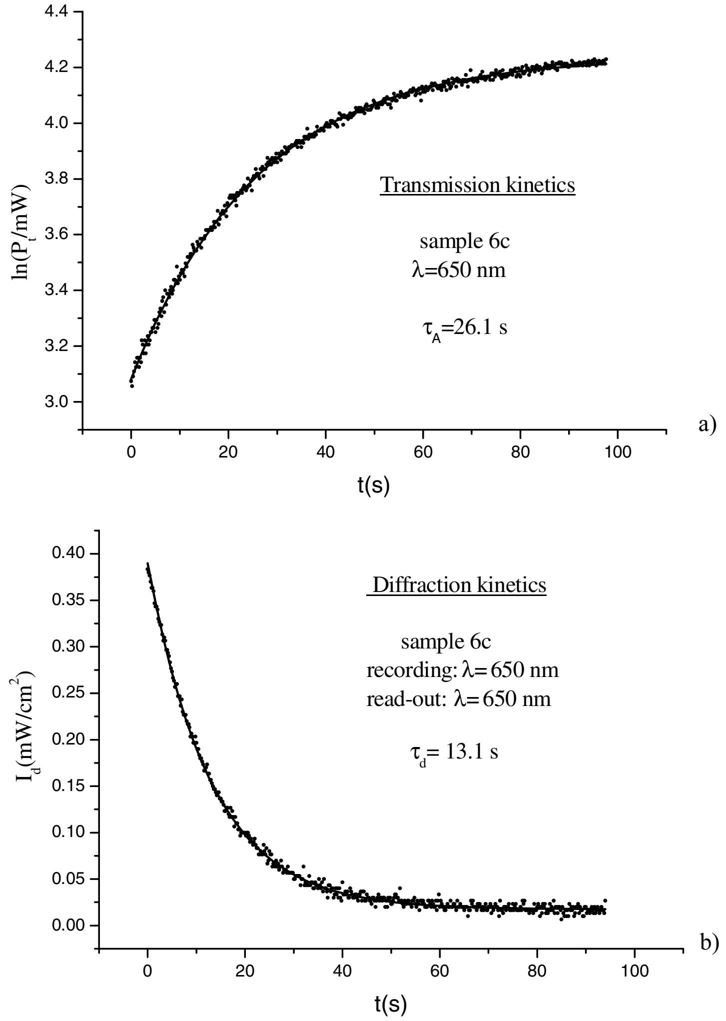

Fig. 4 Transmission (a) and diffracted intensity (b) measured as a function of time for sample 6c at $\lambda = 650$ nm and a readout intensity (= irradiation intensity) of 32 mW/cm^2.

The same series of experiments has been repeated using a He–Ne laser to determine the photochemical rate constant at 633 nm. The reason why we report the obtained results here is mainly to point out possible systematic errors when performing kinetic measurements in a situation where the Gaussian beam profile cannot be neglected anymore. The beam cross section in the previous experiments (Fig. 5a) with the laser diode was large (3×10 mm^2) so that a rather homogeneous part could be selected by an iris diaphragm placed behind the sample, as shown in Fig. 2. In contrast, the beam of the He–Ne laser had Gaussian profile with a nominal diameter of only 1.44 mm. Under these conditions the slopes for transmission and diffraction kinetics obtained from plotting the reciprocal time constant versus intensity differ significantly (Fig. 5b). We find $(\tau_A I_0)^{-1} = (1.93 \pm 0.06)$ cm^2/J for transmission and $(2\tau_d I_0)^{-1} = (1.59 \pm 0.06)$ cm^2/J for diffraction. One trivial reason for such discrepancies might obviously be differing initial absorbances. But this can be minimised by taking care that coloring of the samples is carried out long enough so that the samples are sufficiently close to the stationary state.

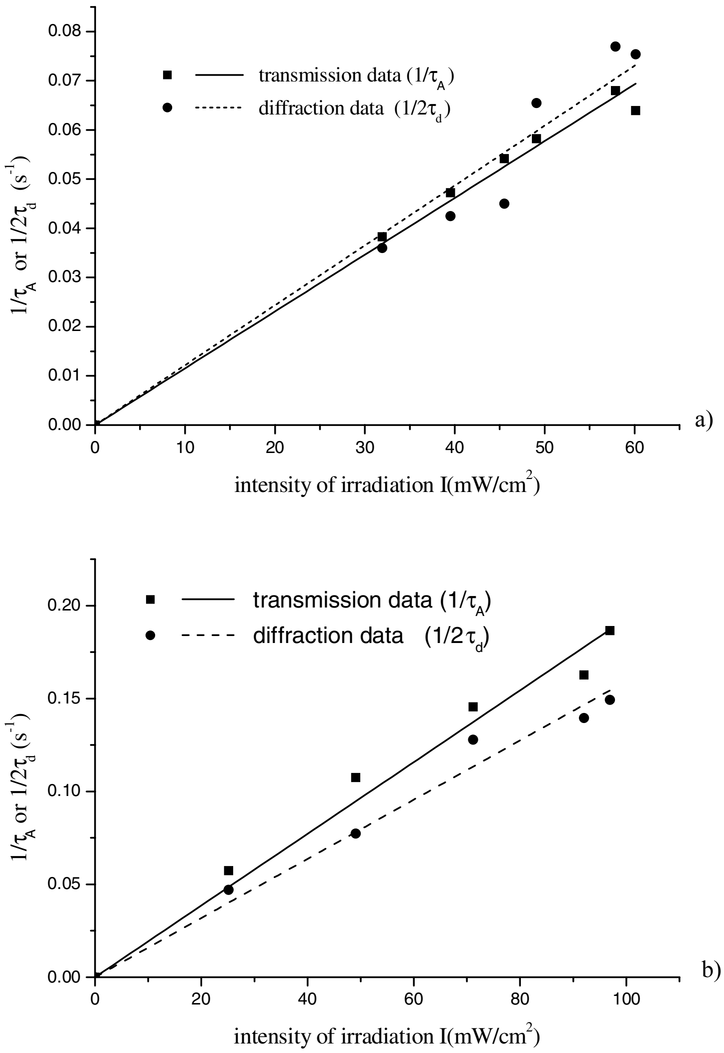

Fig. 5 Plot of $1/\tau_A$ and of $1/2\,\tau_d$ versus intensity for data from transmission (squares) and diffraction experiments (dots), respectively, for sample 6c. Bleaching wavelengths: (a) $\lambda = 650$ nm, (b) $\lambda = 633$ nm. Fitting a linear function to the data (solid line: transmission, dashed line: diffraction) gives the slopes (a) $(\tau_A I_0)^{-1} = (1.15 \pm 0.05)$ cm^2/J from evaluation of transmission data and $(\tau_d I_0)^{-1} = (1.22 \pm 0.05)$ cm^2/J from evaluation of diffraction data, (b) $(\tau_A I_0)^{-1} = (1.93 \pm 0.06)$ cm^2/J for transmission and $(\tau_d I_0)^{-1} = (1.59 \pm 0.06)$ cm^2/J for diffraction.

Another reason is the following: As pointed out in the above theoretical analysis, a pronounced deviation of the beam profile from a homogeneous one may lead to a non-exponential time dependence and thus may falsify the time constants obtained from a single exponential fit. In Fig. 6 we compared a single exponential fit according to Eq. (9) with a fit according to Eq. (11) to the data of a bleaching experiment at 633 nm. To be precise, the fit model was $P_d(t) = P_d(0)\,[1 - \exp(-(t - t_0)/\tau_d)]\,\tau_d/(t - t_0)$ with $P_d(0)$, t_0 and τ_d being free fit parameters. While deviations are seen for Eq. (9), it is obvious, that Eq. (11) matches the data perfectly. We repeated the comparison for several varying conditions with beams of Gaussian profile and always obtained a better, if not a perfect fit when using Eq. (11).

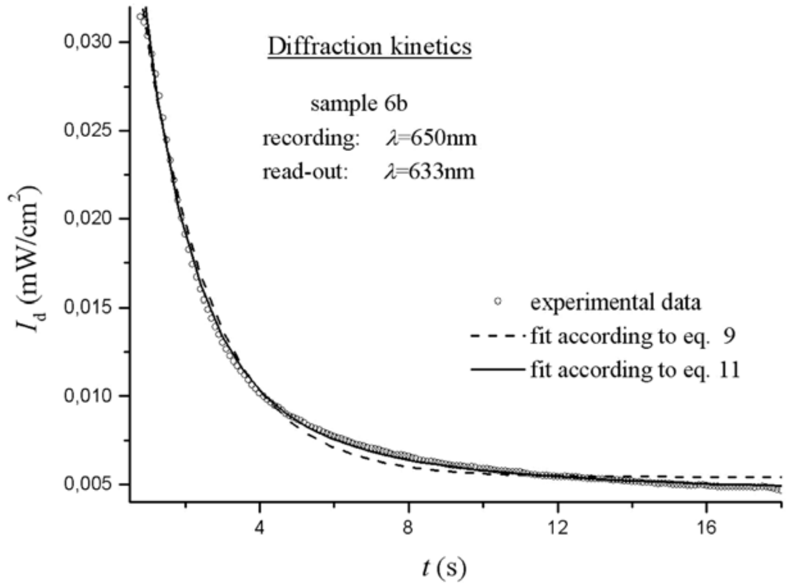

Fig. 6 Diffracted intensity efficiency measured as a function of time for sample 6b at $\lambda = 633$ nm and an intensity of 18.4 mW/cm^2 for read-out and bleaching. Dots: averaged experimental data, dashed line: single exponential fit according to Eq. (9), solid line: fit according to the mathematical model defined by Eq. (11).

5 Discussion

Although there is much literature on fulgides, a comparison of our results with results published on other fulgide systems turned out to be possible only in one case.

Most holographic studies we found in literature measured the diffraction efficiency versus exposure time during writing but do not report on holographic decay experiments [7, 12–19]. In those studies where holographic decay during homogeneous irradiation was monitored no attempt for an analysis of the decay kinetics was made [8, 20]. Hence literature data on the photochemical kinetics deduced from holographic methods are not available.

In contrast, there are many reports using the method of time-resolved transmission spectroscopy. Lessard et al. [13, 18], Lafond et al. [12, 21], and Tork et al. [22, 23] reported on the bleaching and coloring kinetics of furyl-adamantylidene fulgide (Aberchrome 670) doped into several different polymeric host matrices. Some results were given by Kardinahl and Franke on furyl-methylidene fulgide (Aberchrome 540) in a PMMA matrix [17], by Francini et al. on an undefined fulgide [19], by Seibold and Port on isopropylidene fulgide [24], and by Belfield et al. [25] on indoly fulgide.

Since the last-mentioned four groups have not made a serious attempt to analyze the data quantitatively with respect to photochemical kinetics, we will not consider them further. With one exception, namely Ref. [21], all other investigations [12, 13, 18, 22, 23] evaluate the photoreaction rate from their data without giving information on the intensity of the irradiation for bleaching. This makes the values useless for a comparison. Even a comparison between the rate constants k_{UV} for coloring by ultraviolet radiation and k_{VIS} for bleaching by visible radiation, one of the main results in [13, 18] (the same data were published in both papers), has no meaning without comparison of the intensities.

Lafond et al. [21] report a photoreaction rate $k_A = 2.43 \times 10^{-3}$ s^{-1} for bleaching of Aberchrome 670 in PMMA at $\lambda = 514$ nm, $I_0 = 0.292$ mW/cm^2 and for $\Delta A_{e0} \approx 1.9$. From these data we calculate the photochemical reaction constant $\gamma(514\text{ nm}) = 19$ cm^2/J. From their results on Aberchrome 670 in PVK one gets $\gamma(514\text{ nm}) = 21$ cm^2/J. This can be compared with our results, namely $\gamma(650\text{ nm}) = (3.9 \pm 0.3)$ cm^2/J for the photochemical reaction constant of indoly-benzylfulgimide in PMMA. The error in our result refers to the statistical error and is of comparable magnitude with the additional error for the determination of the absolute intensity (see Section 2), i.e. the total relative error of the measurement is approximately 20%. Since the results of Lafond et al. indicate an influence of the host matrix, we compare the values for PMMA which are of the same order of magnitude, but γ being significantly smaller, namely by a factor 5 for indoly-benzylfulgimide. This does, however, not necessarily imply that our photochromic system is slower, because the measurements of Lafond et al. [21] were made much closer to the band maximum of the C-isomer than our measurements.

At 633 nm we find $(\tau_A I_0)^{-1} = (1.93 \pm 0.06)$ cm^2/J for transmission and $(2\tau_d I_0)^{-1} = (1.59 \pm 0.06)$ cm^2/J for diffraction. First of all, both values are somewhat larger than the one measured for 650 nm. Partially one could explain this by the absorption at 633 nm being higher than at 650 nm. However on the other hand 633 nm is closer to the band maximum of the C-isomer. But the main reason not to interpret the measurements further is the fact that the deviation of the values from each other is about 20% and thus larger than the statistical error of about 4%. This indicates a possible systematic error. The origin seems to be the usage of beams with Gaussian profile. So our results at 633 nm cannot be considered as conclusive since our equipment did not permit measurements at 633 nm with expanded beams to avoid the problem.

6 Conclusions

For a photochromic medium with photochemical first order kinetics neither absorbance nor diffraction decay can be expected to be strictly exponential because of the decay of the intensity with penetration depth. Nevertheless, at the beginning the curves decay exponentially to good approximation.

A comparison of kinetic data from transmission and diffraction experiments has confirmed the relationship $\tau_d = \tau_A/2$ between the time constants for absorbance and diffraction decay.

The effect of initial absorbance can appropriately be taken into account by Eq. (5). Thus we obtain $\gamma(650\text{ nm}) = (3.9 \pm 0.3)$ cm^2/J for the photochemical reaction constant of indoly-benzylfulgimide in PMMA which is still in the same order of magnitude as the value $\gamma(514\text{ nm}) = 19$ cm^2/J calculated from the data of Lafond et al. [21] for furyl-adamantylidene fulgide in PMMA.

If Gaussian beams are used in holographic diffraction experiments, the decay is described by a non-exponential law, namely Eq. (11). A remarkable property, namely that Eq. (11) does not depend on the width parameter, makes the determination of the photochemical reaction constant as easy as for experiments with homogeneous intensity distribution, because it is sufficient to analyse the time dependence of the diffracted power.

Acknowledgement This work was partially supported by the Austrian Science Foundation, project FWF P-15642, the Natural Science Foundation of China, project 60337020, and the scientific-technical cooperation project of the ÖAD.

References

[1] S. Kurita, A. Kashiwagi, Y. Kurita, H. Miyasaka, and N. Mataga, Chem. Phys. Lett. **171**, 553 (1990).
[2] Y. Yokoyama, Chem Rev. **100**, 1717 (2000).
[3] M. Seibold, H. Port, and K. Gustav, Chem. Phys. Lett. **314**, 65 (1999).
[4] M. Seibold, M. Handschuh, H. Port, and H. C. Wolf, J. Lumin. **72–74**, 454 (1997).
[5] Y. Yokoyama, H. Hayata, H. Ito, and Y. Kurita, Bull. Chem. Soc. Jpn. **63**, 1607 (1990).
[6] M. Lei, B. Yao, Y. Chen, Y. Han, C. Wang, Y. Wang, N. Menke, G. Chen, and M. Fan, Proc. SPIE **5060**, 28 (2002).
[7] T. Kardinahl and H. Franke, Proc. SPIE **1985**, 742 (1993).
[8] T. Kardinahl and H. Franke, Proc. SPIE **2025**, 574 (1993).
[9] P. Jones, P. Darcy, G. S. Attard, and G. Williams, Mol. Phys. **67**, 1053 (1989).
[10] R. A. Rupp, Y. Zheng, Y. Wang, W. Dong, N. Menke, B. Yao, W. Zhao, Y. Chen, M. Fan, J. Xu, and M. Fally, Absorbance kinetics of dye-doped systems with photochemical first order kinetics, in preparation.

Original

Paper

[11] H. Kogelnik, Bell Syst. Tech. J. **48**, 2909 (1969).
[12] C. Lafond, A. Tork, R. A. Lessard, and M. Bolte, Proc. SPIE **4087**, 732 (2000).
[13] R. A. Lessard, A. Tork, C. Lafond, M. Bolte, and A. Ritcey, Proc. SPIE **3939**, 94 (2000).
[14] C. Lafond, O. Pouraghajani, M. Bolte, M. Bolte, A. Ritcey, and R. A. Lessard, Proc. SPIE **4296**, 226 (2001).
[15] N. Menke, B. Yao, Y. Wang, Y. Zheng, M. Lei, G. Chen, Y. Chen, M. Fan, Y. Han, and X. Meng, Acta Photonica Sin. **32**, 819 (2003).
[16] T. Kardinahl and H. Franke, Proc. SPIE **2212**, 346 (1994).
[17] T. Kardinahl and H. Franke, Appl. Phys. **61**, 23 (1995).
[18] R. A. Lessard, C. Lafond, F. Ghailane, M. Bolte, A. Tork, and I. Petkov, Proc. SPIE **3897**, 46 (1999).
[19] F. Francini, G. Ottavi, P. Sansoni, and B. Tiribilli, Opt. Commun. **130**, 235 (1996).
[20] C. Lafond, M. Bolte, and R. A. Lessard, Proc. SPIE **4833**, 584 (2002).
[21] C. Lafond, R. A. Lessard, M. Bolte, and I. Petkov, Proc. SPIE **3417**, 216 (1998).
[22] A. Tork, C. Lafond, O. Pouraghajani, M. Bolte, A. Ritcey, and R. A. Lessard, Opt. Eng. **41**, 2310 (2002).
[23] A. Tork, T. V. Galstian, and R. A. Lessard, Proc. SPIE **4342**, 593 (2002).
[24] M. Seibold and H. Port, Chem. Phys. Lett. **252**, 135 (1996).
[25] K. D. Belfied, Y. Liu, R. A. Negres, M. Fan, G. Pan, D. J. Hagan, and F. E. Hernandez, Chem. Mater. **14**, 3663 (2002).

